

Article

Development of ELISA-Like Fluorescence Assay for Melamine Detection Based on Magnetic Dummy Molecularly Imprinted Polymers

Guangyang Liu ^{1,2,†}, Yongxin She ^{2,†}, Sihui Hong ², Jing Wang ^{2,*} and Donghui Xu ^{1,*}

¹ Institute of Vegetables and Flowers, Chinese Academy of Agricultural Sciences, Key Laboratory of Vegetables Quality and Safety Control, Ministry of Agriculture of China, Ministry of Agriculture, Beijing 100081, China; liuguangyang@caas.cn

² Institute of Quality Standard and Testing Technology for Agro Products, Chinese Academy of Agricultural Sciences, Key Laboratory of Agrifood Safety and Quality, Ministry of Agriculture of China, Beijing 100081, China; sheyongxin0891@126.com (Y.S.); sihuihong2016@126.com (S.H.)

* Correspondence: W_jing2003@126.com (J.W.); xudonghui@caas.cn (D.X.)

† Co-authors with equal contributions.

Received: 5 February 2018; Accepted: 3 April 2018; Published: 4 April 2018



Featured Application: The developed method would be useful for monitoring melamine in milk and formula powdered milk.

Abstract: We present a directly competitive fluorescence assay for highly sensitive detection of melamine in milk using magnetic dummy molecularly imprinted polymers (MDMIPs). The detection principle is based on competitive binding between the fluorescent label and melamine on the MDMIPs. The fluorescent label was obtained by combining fluorescein isothiocyanate (FITC) with melamine in ethanol and water. MDMIPs were prepared on the surface of Fe₃O₄@SiO₂ nanoparticles using 2,4-diamino-6-methyl-1,3,5-triazine as dummy template. The MDMIPs were characterized and their adsorption capacity was evaluated based on their static adsorption and Scatchard analysis. Results suggest that MDMIPs were successfully coated on the Fe₃O₄@SiO₂ surface and had a core-shell structure. Adsorption experiments suggested that the MDMIPs had higher specific recognition capacities for melamine and FITC-melamine (FITC-Mel) than did magnetic dummy molecularly non-imprinted polymers. Competitive binding between FITC-Mel and melamine was performed under the optimum conditions to determine melamine quantitatively. The linear range of this fluorescence assay was 0.1–20 mg/L for melamine detection. The detection limit was 0.05 mg/L in negative milk samples. The assay was also successfully employed to detect melamine in spiked milk samples, with satisfactory recoveries, i.e., between 70.2% and 92.7%.

Keywords: ELISA-like fluorescence assay; magnetic dummy molecularly imprinted polymers; 2,4-diamino-6-methyl-1,3,5-triazine; fluorescein isothiocyanate; melamine

1. Introduction

Molecular imprinting techniques have attracted research interest globally in recent years [1–4]. Molecularly imprinted polymers (MIPs) have many advantages over other recognition systems, e.g., low cost and easy synthesis, high stability under harsh chemical and physical conditions, and excellent reusability [5]. Consequently, MIPs have been used in many fields, including solid-phase extraction [6–8], drug delivery [9,10], catalysis [11], and sensing [12,13]. However, the traditional methods of MIP preparation have a number of drawbacks, e.g., incomplete template removal,

low rebinding capacity, poor template accessibility, slow mass transfer, and difficult solid–liquid separation [14,15].

Surface molecular imprinting on various surfaces, including SiO₂ nanoparticles [16], carbon materials [17], polymeric supports [18], metal oxide particles [19], and magnetic materials [20], has been used to overcome these problems. Magnetic nanoparticles have been widely used in the preparation of magnetic molecularly imprinted polymers (MMIPs) because of their properties such as small size, high magnetic susceptibility, and high surface-to-volume ratio. MMIPs can be easily separated from a complex matrix using an external magnet, enabling convenient and efficient preconcentration to avoid using time-consuming solid-phase extraction and column packing [21,22]. Potential interference from leakage of residual template molecules embedded in MIPs can be prevented by using a dummy molecular imprinting technique, in which a structural analog of the target compound is used as a template for MIP preparation [23].

Melamine, which is a triamine and contains a nitrogen heterocyclic ring, is an important organic chemical; it is used in the production of melamine resins, which are widely used in wood processing, plastics, paints, papermaking, textiles, leather, electrical goods, and medicines [24]. Melamine detection became a hot topic after cases of infant kidney stones caused by melamine-poisoned infant formula powders in China, and pet deaths from melamine-poisoned feeds in USA [25,26]. Melamine had been illegally added to infant formula powders, dairy products and pet feeds to enhance the protein content measured by the Kjeldahl method. Since 2008, the Chinese government has forbidden the artificial addition of melamine to any food, and the temporary limitation of the volume of melamine in liquid milk is 0.05 mg/Kg. Analytical methods such as high-performance liquid chromatography (HPLC) [27], gas chromatography-mass spectrometry (GC-MS) [28], HPLC-MS/MS [29], surface-enhanced Raman scattering [30], electrochemical immunosensing [31], and enzyme-linked immunoassays (ELISA) [32] have been used for melamine determination. Although these analytical methods are highly sensitive, selective, and efficient, they are time consuming, expensive, and need sophisticated instruments and highly skilled personnel.

Fluorescent sensors provide a promising method for the detection of trace pollutants because such methods are simple, rapid, and have high sensitivity and selectivity [33,34]. The use of combinations of MIPs and fluorescence assays to detect melamine in milk and infant formula milk powder has been reported [35–37]. Fluorescent MIP sensors can be divided into two categories based on their preparation method. In the first method, fluorescent materials such as a fluorescent functional monomers or quantum dots are used for molecular imprinting. The interactions between template molecules and the fluorescent functional monomers or quantum dots in the MIPs cause changes in the fluorescence signals, which can be monitored to detect target molecules quantitatively [38,39]. However, the synthesis and modification of fluorescent functional monomers are complicated and quantum dots cannot be uniformly embedded into MIPs. These problems prevent the widespread use of this type of fluorescent MIP sensor. The other method combines the binding properties of MIPs (plastic antibodies) with a competitive fluorescence assay, similar to fluorescence ELISA [2,40–42]. For example, our research group designed a novel fluorescent MIP sensor involving direct competitive binding between triazine herbicide and 5-(4,6-dichlorotriazinyl)aminofluorescein on MMIPs for atrazine detection in tap water [2].

Based on the above, we designed a novel magnetic dummy molecularly imprinted polymer (MDMIP) for fluorescence detection of melamine in milk. The principle is based on competitive absorption between a melamine molecule and a fluorescein isothiocyanate (FITC)–melamine (FITC-Mel) conjugate on the surface active sites of the MDMIPs. The MDMIPs were prepared on the surfaces of Fe₃O₄@SiO₂ to absorb specifically melamine molecules. The MDMIPs were characterized, and their adsorption capacity was evaluated based on their static adsorption and Scatchard analysis. Competitive binding between FITC-Mel and melamine was used for quantitative detection of melamine in spiked milk samples. Compared to the above-mentioned melamine detection methods, the detection method established in this paper needs no sophisticated experimental procedure and instruments.

In addition, the present competitive fluorescence assay based on MDMIP is simpler than current Quantum Dots-MIP (QDs-MIP) fluorescent sensors with embedding of fluorescent QDs into the MIPs.

2. Materials and Methods

2.1. Reagents and Apparatus

$\text{FeCl}_3 \cdot 6\text{H}_2\text{O}$, poly(ethylene glycol) (PEG 1000), 2,2-azobis(isobutyronitrile) (AIBN), tetraethoxysilane (TEOS), ethylene glycol dimethacrylate (EGDMA) and methacrylic acid (MAA) were purchased from Aladdin Industrial Corporation (Shanghai, China). Ammonium hydroxide, ethylene glycol, 2,4-diamino-6-methyl-1,3,5-triazine, 3-(trimethoxysilyl)propyl methacrylate (MPS), anhydrous ethanol, anhydrous methanol and HPLC-grade anhydrous acetonitrile, acetic acid, and sodium acetate were purchased from Sinopharm Chemical Reagent Co., Ltd. (Shanghai, China).

Transmission electron microscopy (TEM; JEM-1200EX, JEOL, Tokyo, Japan), vibration sample magnetometry (VSM; EV7, ADE, Waltham, MA, USA), Fourier-transform infrared (FT-IR) spectroscopy (FT-IR 100, Perkin Elmer, Waltham, MA, USA), HPLC (Waters 2695 system with 2998 photodiode array detector); HPLC-MS/MS (Agilent 1100 system with API-2000 mass spectrometer, Santa Clara, CA, USA; AB SCIEX (Shanghai, China), and a multimode reader (Tecan infinite 200 pro, Mannedorf, Switzerland) were used.

2.2. MDMIP Synthesis

Fe_3O_4 nanoparticles were prepared using a modified version of a previously reported hydrothermal method [43]. $\text{FeCl}_3 \cdot 6\text{H}_2\text{O}$ (0.665 g), anhydrous sodium acetate (1.80 g), PEG 1000 (0.5 g), and ethylene glycol (20 mL) were placed in a Teflon-lined stainless-steel autoclave. The autoclave was heated at 180 °C for 8 h. The Fe_3O_4 nanoparticles were separated magnetically and washed several times with ethanol and water. The precipitate was dried at 60 °C in a vacuum oven.

The Fe_3O_4 particles were modified with SiO_2 using the method reported by Ni et al. [44]. Fe_3O_4 (200 mg) was dispersed in 0.1 M hydrochloric acid solution (50 mL) by sonication for 10 min. The Fe_3O_4 was separated using an external magnet and mixed with ethanol (160 mL) and ultrapure water (40 mL) by sonication for 15 min. Ammonium hydroxide (5.0 mL, 25 wt %) and TEOS (0.7 mL) were then added sequentially. The mixture was stirred at 40 °C for 12 h. The $\text{Fe}_3\text{O}_4@ \text{SiO}_2$ nanoparticles were collected magnetically, thoroughly washed with ethanol and water, and dried in a vacuum for 24 h.

The $\text{Fe}_3\text{O}_4@ \text{SiO}_2$ nanoparticles were modified with vinyl groups. The nanoparticles (200 mg) were dissolved in methanol (50 mL) by sonication for 15 min, followed by addition of MPS (3 mL). The mixture was incubated at room temperature for 24 h. The $\text{Fe}_3\text{O}_4@ \text{SiO}_2@ \text{MPS}$ nanoparticles were separated using an external magnet, washed with water, and dried in a vacuum for 24 h.

The MDMIPs were prepared using the surface molecular imprinting method [45]. Typically, 0.25 mm 2,4-diamino-6-methyl-1,3,5-triazine and 1 mm MAA were dispersed in chloroform (30 mL) containing dimethyl sulfoxide (1 mL) and ethylene glycol (2 mL) by sonication for 15 min, and the mixture was cultivated at 4 °C for 3 h. Acetonitrile (10 mL) containing $\text{Fe}_3\text{O}_4@ \text{SiO}_2@ \text{MPS}$ nanoparticles (80 mg) was mixed and then ultrasonicated for 30 min.

EGDMA (5 mm) and AIBN (25 mg) were then added sequentially to the mixture. The solution was deoxygenated with N_2 for 10 min and the reaction was performed at 60 °C for 24 h, with mechanical stirring. The MDMIPs were separated magnetically and washed with methanol/acetic acid (9:1, v/v) until no template was found by HPLC. Magnetic dummy molecularly non-imprinted polymers (MDNIPs) were prepared using the same procedures but without the dummy template. The procedure for MDMIP preparation is shown in Figure 1A.

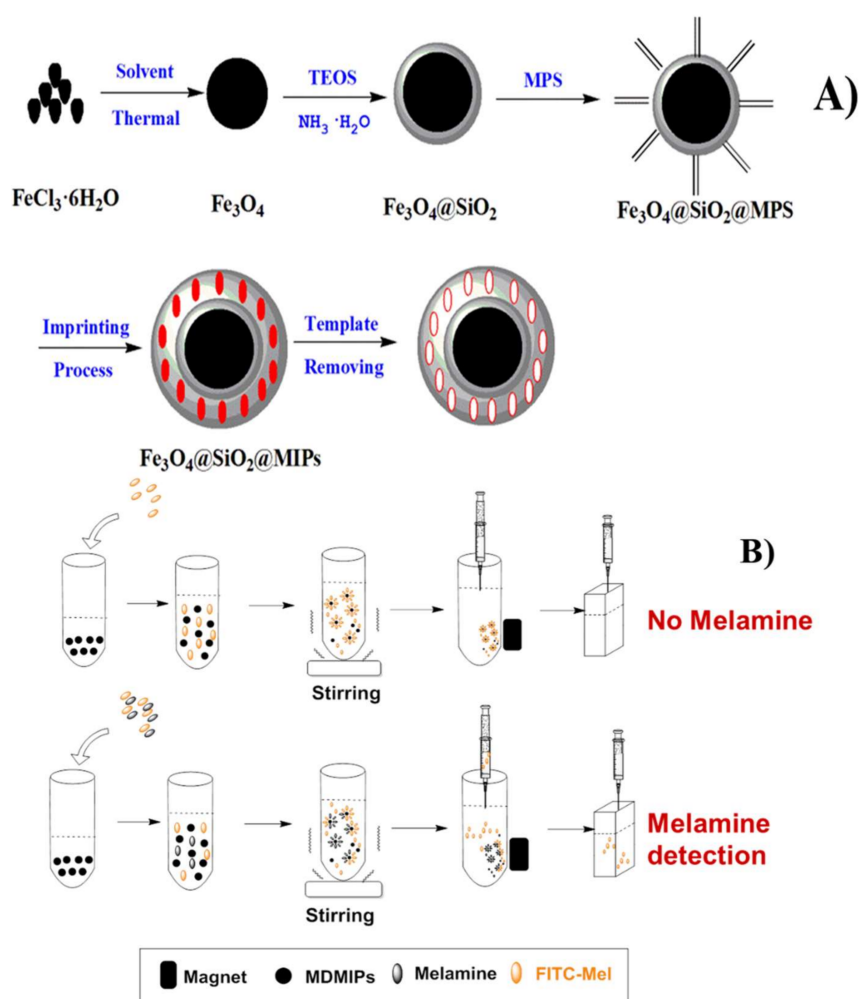


Figure 1. (A) Procedure for MDMIP preparation and (B) mechanism of competitive fluorescence assay of melamine.

2.3. Synthesis of FITC-Mel Fluorescent Label

FITC-Mel was synthesized using a modified version of a previously reported method [46]. Melamine (20 mg) was dissolved in ethanol (15 mL) by sonication for 15 min, followed by addition of FITC (20 mg). The mixture was stirred for 24 h at room temperature in the dark. The product was purified by cation-exchange solid-phase extraction and the purified FITC-Mel was identified using electrospray ionization MS (ESI-MS).

2.4. Characterization of MDMIPs

The MDMIP morphology and size were examined using TEM. FT-IR spectra of solid samples dispersed in KBr powder were recorded in the range $400\text{--}4000\text{ cm}^{-1}$. The magnetization was measured at room temperature using vibrating sample magnetometer (VSM).

Adsorption Experiments

The adsorption capacity and selectivity of the MDMIPs were investigated by performing static adsorption experiments. MDMIPs or MDNIPs (2 mg) were added to a 2 mL polyethylene tube containing melamine solutions (1 mL) of various concentrations (0.1–20 mg/L). After incubation for 2 h at room temperature, the MDMIPs or MDNIPs were collected using an external magnet and the supernatant solutions were examined using HPLC. The static binding capacities of the MDMIPs and

MDNIPs in melamine adsorption were calculated using the equation $Q = (C_0 - C_e) \times V/M$, where Q is the static binding capacity, C_0 is the initial melamine concentration, C_e is the equilibrium concentration of melamine, V is the total volume of the initial melamine solution, and M is the mass of MDMIPs or MDNIPs.

The binding capacity and binding site properties were studied by Scatchard analysis using the equation $Q/C_e = (Q_{\max} - Q)/K_D$, where C_e is the equilibrium concentration of the analyte, K_D is the dissociation constant, and Q_{\max} is the maximum amount of apparent binding. Plots with Q/C_e as the ordinate and Q as the abscissa enabled identification of the types of binding sites, and K_D and Q_{\max} were calculated based on the linear regression curves and corresponding equations.

2.5. Fluorescence Measurements

Fluorescence detection was performed at an excitation wavelength of 478 nm and the emission was recorded from 490 to 800 nm. After template removal, MDMIPs (2 mg) were mixed with a methanol solution (1 mL) containing FITC-Mel (2.08 mg/L) and various concentrations of melamine. The mixture was shaken at room temperature in the dark for 2 h. The supernatant was separated using an external magnetic field. The fluorescence intensity of the supernatant solution was monitored using a microplate reader. The mechanism of competitive fluorescence assay of melamine is shown in Figure 1B.

2.6. Preparation of Milk Samples

Blank milk samples (1 g) were spiked with melamine at levels of 0.25, 0.5, 1.0 and 25 mg/kg. The spiked milk was mixed with acetonitrile (9 mL) and the solution was vortexed, then sonicated for 15 min, and centrifuged at 10,000 rpm for 5 min. The supernatant was purified using a PCX-SPE cartridge, as previously reported [47]. The cartridge was first conditioned with methanol (3 mL) and deionized water (5 mL). The milk sample (5 mL) was diluted with water (5 mL). The diluted sample was passed through the cartridge and then the cartridge was washed with methanol (3 mL) and deionized water (3 mL) to remove matrix interference. The analyte was recovered by eluting the cartridge with 5% ammonium hydroxide in methanol (6 mL). The eluate was evaporated to dryness and the residues were redissolved in methanol (1 mL). The analyte solution was filtered through a 0.22 μm poly(vinylidene fluoride) filter membrane and subjected to competitive fluorescence analysis.

The potential use of this competitive fluorescence assay in practical applications was evaluated based on the recoveries from the spiked milk samples. As a reference, HPLC-MS/MS was used to determine the recovery values and relative standard deviations (RSDs) of the spiked milk samples.

3. Results and Discussion

3.1. Mass Spectrum of FITC-Mel

FITC-Mel was examined using ESI-MS in positive- and negative-ion modes. The molecular weights of FITC and melamine are 389.38 and 126.12, respectively. Figure 2 shows that FITC-Mel has three hydroxyl and two amino groups. In positive-ion mode, the molecular ion peak should appear at 516.5 ($M + H$)⁺ or 517.5 ($M + 2H$)²⁺, but we did not observe this molecular ion peak. In negative-ion mode, the molecular ion peak should appear at 514.5 ($M - H$)⁻, 513.5 ($M - 2H$)²⁻, or 512.5 ($M - 3H$)³⁻. Figure 2 shows a molecular ion peak at 512.8, corresponding to FITC-Mel and indicating successful combination of FITC and melamine. In the previous literature [48], a commercial fluorescent, 5-(4,6-dichlorotriazinyl) amino fluorescein (DTAF) was used as fluorescent label and structural analog to monitor melamine by performing directly competitive adsorption. However, there is a relatively large difference in structure between DTAF and melamine, which restricts the sensitivity and selectivity of the fluorescent assay. In this work, we prepared FITC-Mel as a novel fluorescent label by combining FITC and melamine using chemical modification. The structure of

FITC-Mel has a melamine molecule which will endows it high similarity and provides the fluorescent MIP sensor developed in this paper with good recognition and sensitivity.

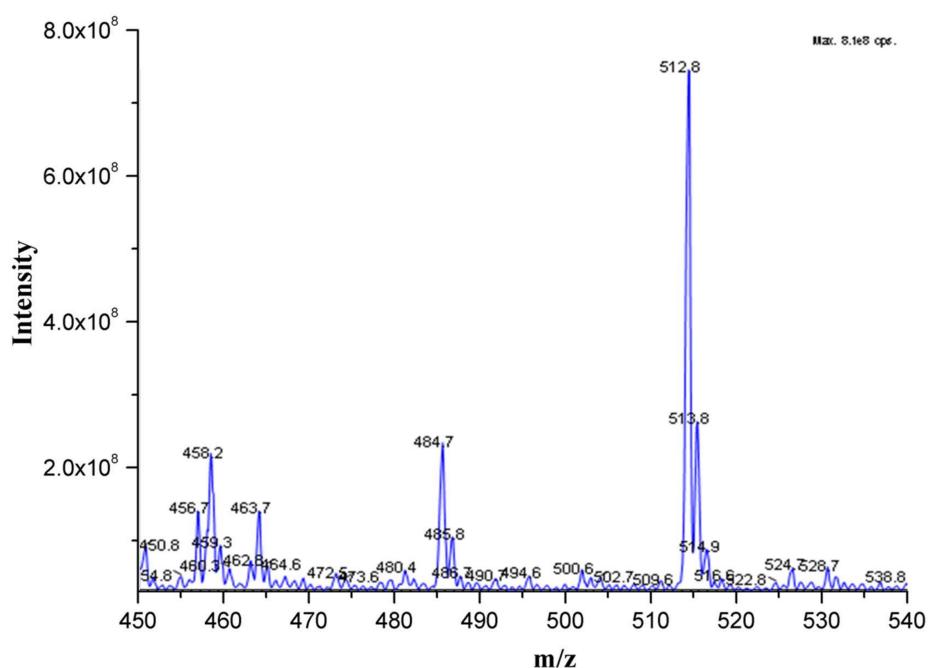


Figure 2. MS/MS spectra of FITC-Mel in negative-ion mode.

3.2. MDMIP Characterization

Figure 3 shows TEM images of Fe_3O_4 , $\text{Fe}_3\text{O}_4@\text{SiO}_2@\text{MPS}$, and the MDMIPs. The figure shows that Fe_3O_4 was monodispersed, with a mean diameter of 20 nm and a uniform size distribution. Figure 3b shows that the diameter of $\text{Fe}_3\text{O}_4@\text{SiO}_2@\text{MPS}$ was approximately 300 nm; this confirms that SiO_2 and MPS layers were uniformly coated on Fe_3O_4 . After imprinting, the MDMIP diameter was about 400 nm, which suggests successful synthesis of core-shell MDMIPs.

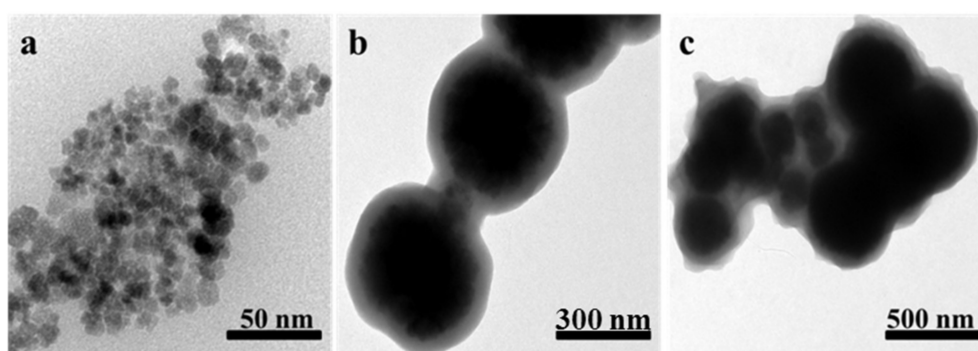


Figure 3. TEM images of (a) Fe_3O_4 ; (b) $\text{Fe}_3\text{O}_4@\text{SiO}_2$; and (c) MDMIPs.

Figure 4A shows the FT-IR spectra of Fe_3O_4 , $\text{Fe}_3\text{O}_4@\text{SiO}_2@\text{MPS}$, and the MDMIPs. A peak at 579.8 cm^{-1} , attributed to the Fe–O stretching vibration, appears in all the spectra. This shows that the Fe_3O_4 nanoparticles were successfully coated with the polymer. The spectrum of $\text{Fe}_3\text{O}_4@\text{SiO}_2@\text{MPS}$ shows peaks from Si–O–Si, at 1087.1 cm^{-1} , Si–O–H, at 955 cm^{-1} , and S–O, at 802 cm^{-1} . These results indicate the formation of SiO_2 shells on the Fe_3O_4 surfaces. The peak at 1622.9 cm^{-1} in the $\text{Fe}_3\text{O}_4@\text{SiO}_2@\text{MPS}$ spectrum is attributed to the C=C stretching vibration, indicating successful

modification of the $\text{Fe}_3\text{O}_4@SiO_2$ nanoparticles with vinyl groups. The C=O and C–O peaks, at 1733 and 1255 cm^{-1} , respectively, in the MDMIP spectrum indicate that EGDMA and MAA were successfully imprinted on the surfaces of the $\text{Fe}_3\text{O}_4@SiO_2@MPS$ nanoparticles.

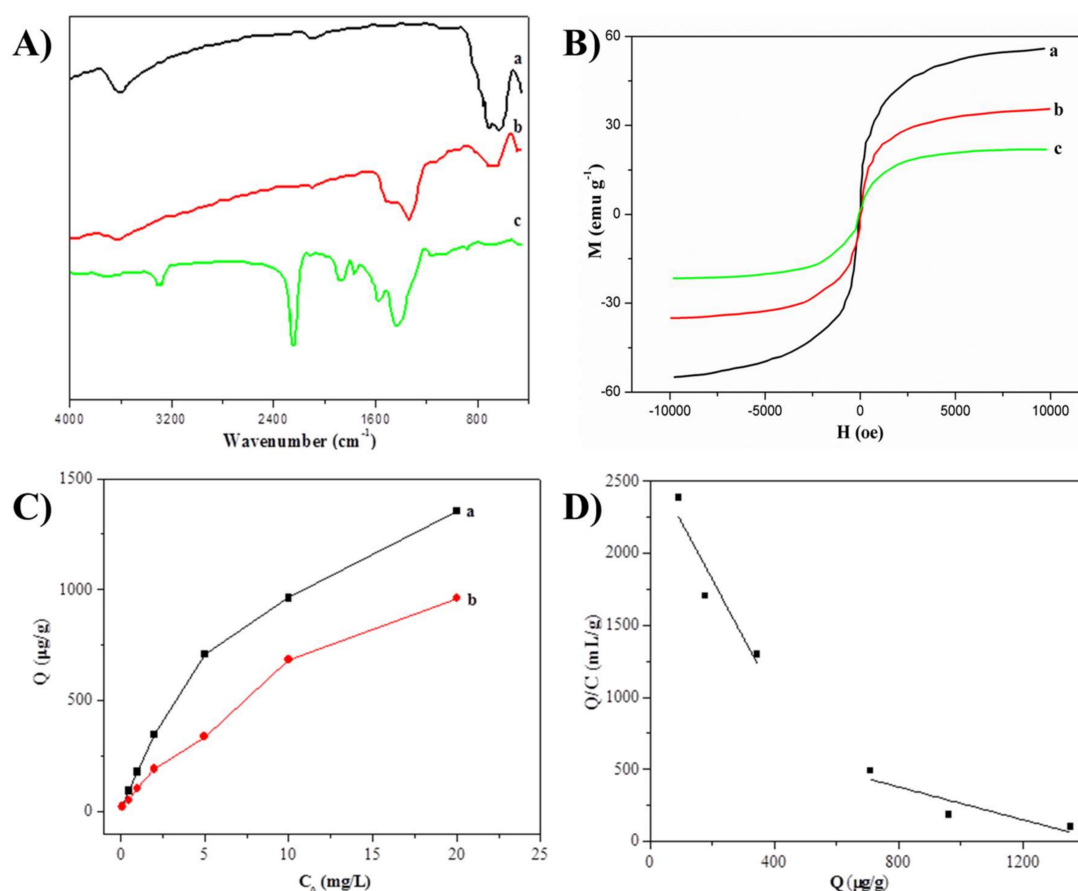


Figure 4. (A) FT-IR spectra of Fe_3O_4 (a), $\text{Fe}_3\text{O}_4@SiO_2$ (b) and MDMIPs (c); (B) Magnetization curves for Fe_3O_4 (a), $\text{Fe}_3\text{O}_4@SiO_2$ (b), and MDMIPs (c); (C) Melamine adsorption isotherms of MDMIPs (a) and MDNIPs (b); (D) Scatchard analysis of melamine adsorption by MDMIPs.

The magnetic properties of Fe_3O_4 , $\text{Fe}_3\text{O}_4@SiO_2@MPS$, and the MDMIPs were studied using VSM. Figure 4B shows that the saturation magnetization values of Fe_3O_4 , $\text{Fe}_3\text{O}_4@SiO_2@MPS$, and the MDMIPs were 55.078, 35.247, and 22.149 emu/g, respectively. The magnetic hysteresis loops show that the remanence and coercivity values were zero, indicating that Fe_3O_4 , $\text{Fe}_3\text{O}_4@SiO_2@MPS$, and the MDMIPs were all superparamagnetic.

3.3. Binding Properties

The isothermal adsorption capacities of the MDMIPs and MDNIPs for melamine are shown in Figure 4C. The amounts of melamine adsorbed on the MDMIPs and MDNIPs increased with increasing initial melamine concentration. The binding capacity of the MDMIPs was higher than that of the MDNIPs. The reason might be that the MDMIPs have specific binding sites that match the size and structure of melamine, whereas the MDNIPs have only non-specific binding sites. Scatchard analysis was used to investigate the adsorption site heterogeneities of the MDMIPs and MDNIPs. Figure 4D shows that the Scatchard plot for melamine adsorption on the MDMIPs was not a single linear plot but two linear plots with different slopes. The slopes and intercepts of the two linear regression curves can be used to calculate K_D and Q_{\max} . The linear regression equation for low initial concentrations was $y = -2.8043x + 2400.1$; the K_D and Q_{\max} values were 0.36 $\mu\text{g}/\text{mL}$ and 855.8 $\mu\text{g}/\text{g}$, respectively.

The linear regression equation for high initial concentrations was $y = -0.5702x + 833.8$; the K_D and Q_{max} values were $1.75 \mu\text{g/mL}$ and 1.46 mg/g , respectively. As shown in Figure 4D, two parts of the Scatchard plot curve indicated there were two types of binding sites, nonspecific and specific binding sites. At the low initial concentration of melamine, MIP showed nonspecific adsorption. However, specific recognition binding sites will be activated at the relative high melamine concentrations.

3.4. Determination of Melamine in Milk Using Fluorescence Assays

Based on its good selectivity and purification ability, an MIP-SPE cartridge was used for solid-phase extraction before the competitive fluorescence assays. Figure 5A shows the competitive binding reaction between FITC-Mel and melamine at various melamine concentrations. Lower melamine adsorption on the MDMIPs resulted in greater FITC-Mel binding to the MDMIPs and a decrease in the fluorescence intensity of the supernatant. Figure 5B shows that the fluorescent intensity of the supernatant increased linearly with the logarithm of the melamine concentration in the range 0.1–20 mg/L. The linear regression equation for the curve was $y = 0.6386x + 0.7098$ and the correlation coefficient (R^2) was 0.9345. The limit of detection was 0.05 mg/L in negative milk samples (signal/noise = 3).

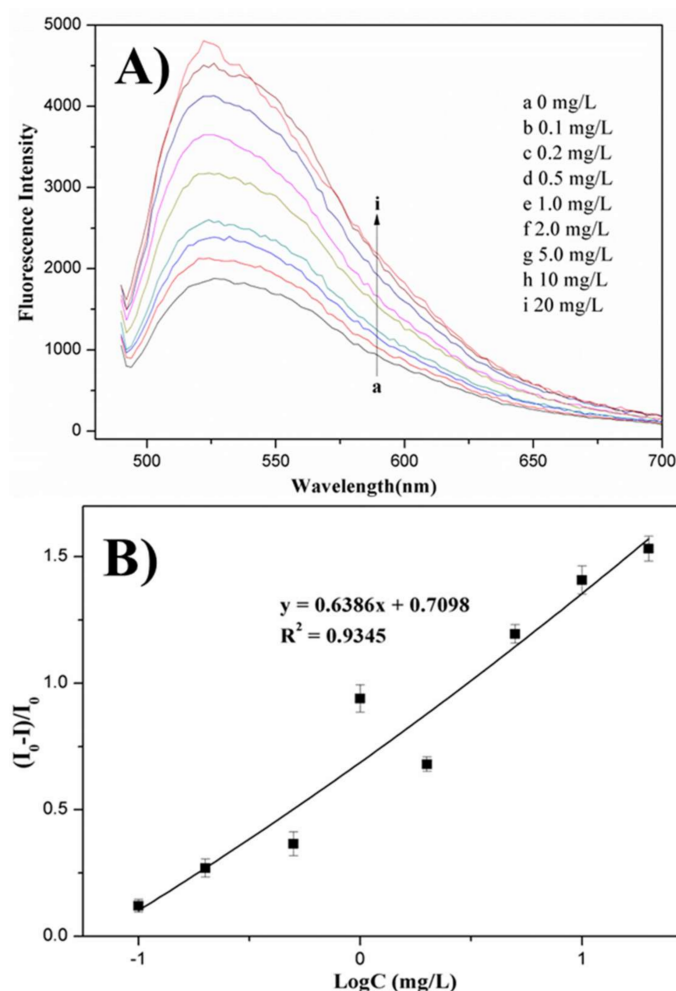


Figure 5. (A) Fluorescence spectra of FITC-Mel with different concentrations of melamine and (B) Standard calibration plots of $(I - I_0)/I_0$ against the logarithm of the melamine concentration from 0.1 to 20 mg/L in milk samples.

To investigate method selectivity, some common potential interfering substances such as dicyandiamide, trazine, cyanuric acid and chloramphenicol were tested by conducting experiments at the same concentration (1.0 mg/L). As shown in Figure 6, only melamine could induce a considerable change of the fluorescence signal at 526 nm. No dramatic changes at 526 nm were observed in the presence of dicyandiamide, trazine, cyanuric acid and chloramphenicol.

Milk samples spiked with different concentrations of melamine (0.25, 0.5, 1.0, and 2.5 mg/L) were pretreated using liquid–liquid extraction and MIP-SPE. The melamine in the spiked milk samples was determined using the developed competitive fluorescence assay. HPLC/MS/MS was also used to determine the melamine recoveries and RSDs for the spiked milk samples. The results are shown in Table 1; the recovery means for melamine in the spiked milk samples were between 70.2% and 92.7%, and the RSD values were in the range 5.4–12.4% ($n = 3$). The successful use of the competitive fluorescence assay to determine melamine in spiked milk samples suggests that the developed method would be useful for monitoring melamine in milk and formula powdered milk.

Table 1. Results for analysis of melamine in milk samples.

Added (mg/L)	Fluorescent Found (mg/L)	Recovery, Means \pm R.S.D (%) ($n = 3$)	HPLC-MS/MS
0.25	0.175	70.2 \pm 8.9	83.5 \pm 4.8
0.5	0.411	82.2 \pm 12.4	82.7 \pm 4.1
1.0	0.853	85.3 \pm 7.6	89.6 \pm 3.3
2.5	2.32	92.7 \pm 5.4	93.5 \pm 2.7

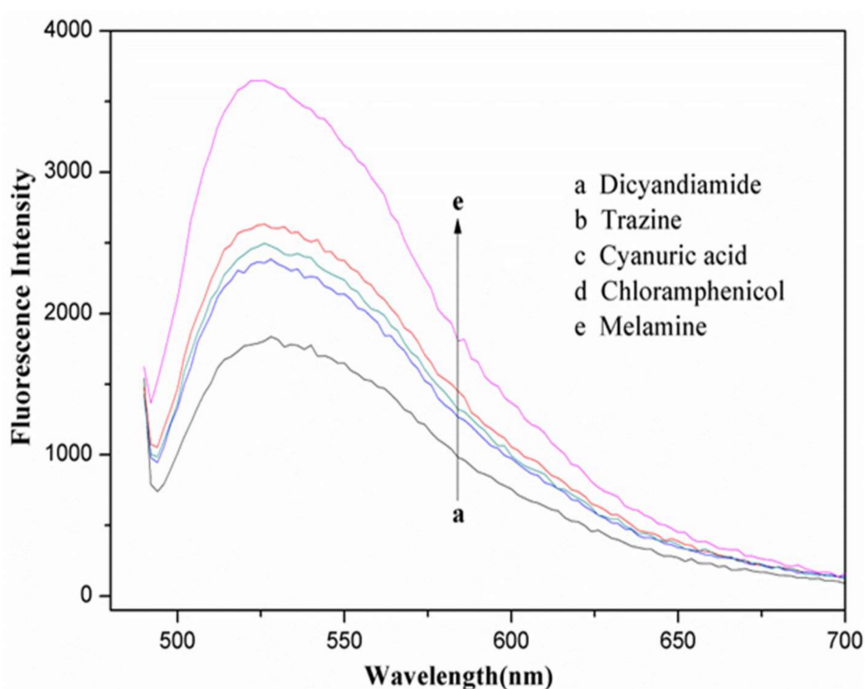


Figure 6. Fluorescence spectra of FITC-Mel with different interfering substances by conducting experiments at the same concentration (1.0 mg/L).

3.5. Comparison

The previous literature reported that a fluorescent competitive detection method based on dummy molecularly imprinted polymers (DMIPs) for melamine was developed [48]. DMIPs were prepared using a traditional molecular imprinting technique, which has some limitations, such as poor binding capacity, incomplete template removal, slow mass transfer and poor selectivity. Compared to conventional MIPs, we synthesized a novel magnetic surface MIP by using $\text{Fe}_3\text{O}_4@\text{SiO}_2$

nanoparticles as a support and magnetic core. The novel MDMIPs have a core-shell sphere structure which enhances the absorption capacity and selectivity for melamine and accelerates the mass transfer. More importantly, most adsorption binding sites were distributed on the surface of MIPs, which indicate a good template removal performance. In addition, MDMIPs possess a high magnetic property that allows for the rapid separation of melamine from the complex sample matrix without any additional operations such as centrifuge.

4. Conclusions

An ELISA-like fluorescence assay for the simple and sensitive detection of melamine in milk was developed. The detection principle of the fluorescence assay was based on competitive binding between melamine molecules and FITC-Mel conjugates on the surface active sites of MDMIPs, similar to fluorescence ELISA. The increase in the fluorescence intensity of the supernatant was linearly related to the logarithm of the melamine concentration in the range 0.1–20 mg/L. The detection limit for melamine in milk was 0.05 mg/L. The MDMIPs in this ELISA-like fluorescence assay are more easily prepared than current fluorescent MIP sensors such as fluorescent functional monomers or quantum dots for molecular imprinting and do not require complicated synthesis and modification. More importantly, the fluorescence assay is easily performed, without the need for professionals, and sophisticated experimental techniques and instrumentation. The results show that this method could be used for the determination of melamine in milk.

Acknowledgments: This work was supported by the National Natural Science Foundation of China (No. 31701695) and the National Key Research Development Program of China (No. 2016YFD0200200).

Author Contributions: Guangyang Liu conceived and designed the experiments; Yongxin She performed the synthesis of all materials; Guangyang Liu and Sihui Hong acquired and analyzed the experimental data; Jing Wang contributed the project idea and reagents; Donghui Xu wrote the paper.

Conflicts of Interest: The authors declared that they have no conflicts of interest to this work. We declare that we do not have any commercial or associative interest that represents a conflict of interest in connection with the manuscript submitted. The founding sponsors had no role in the design of the study; in the collection, analyses, or interpretation of data; in the writing of the manuscript; or in the decision to publish the results.

References

1. Chen, L.; Xu, S.; Li, J. Recent advances in molecular imprinting technology: Current status, challenges and highlighted applications. *Chem. Soc. Rev.* **2011**, *40*, 2922–2942. [[CrossRef](#)] [[PubMed](#)]
2. Liu, G.; Li, T.; Yang, X.; She, Y.; Wang, M.; Wang, J.; Zhang, M.; Wang, S.; Jin, F.; Jin, M. Competitive fluorescence assay for specific recognition of atrazine by magnetic molecularly imprinted polymer based on Fe₃O₄-chitosan. *Carbohydr. Polym.* **2016**, *137*, 75–81. [[CrossRef](#)] [[PubMed](#)]
3. Liu, G.; Li, T.; Yang, X.; She, Y.; Wang, S.; Wang, J.; Zhang, M.; Jin, F.; Jin, M.; Shao, H. Preparation of a magnetic molecularly imprinted polymer using g-C₃N₄-Fe₃O₄ for atrazine adsorption. *Mater. Lett.* **2015**, *160*, 472–475. [[CrossRef](#)]
4. Chen, L.; Wang, X.; Lu, W.; Wu, X.; Li, J. Molecular imprinting: Perspectives and applications. *Chem. Soc. Rev.* **2016**, *45*, 2137–2211. [[CrossRef](#)] [[PubMed](#)]
5. Takeuchi, T.; Sunayama, H. Molecularly Imprinted Polymers. In *Encyclopedia of Polymeric Nanomaterials*; Springer: Berlin/Heidelberg, Germany, 2015; pp. 1291–1295.
6. Ahmadi, M.; Madrakian, T.; Afkhami, A. Solid phase extraction of doxorubicin using molecularly imprinted polymer coated magnetite nanospheres prior to its spectrofluorometric determination. *New J. Chem.* **2015**, *39*, 163–171. [[CrossRef](#)]
7. Pavlović, D.M.; Nikšić, K.; Livazović, S.; Brnardić, I.; Anžlovar, A. Preparation and application of sulfaguanidine-imprinted polymer on solid-phase extraction of pharmaceuticals from water. *Talanta* **2015**, *131*, 99–107. [[CrossRef](#)] [[PubMed](#)]
8. Tian, J.; Bai, J.; Peng, Y.; Qie, Z.; Zhao, Y.; Ning, B.; Gao, Z. A core-shell-structured molecularly imprinted polymer on upconverting nanoparticles for selective and sensitive fluorescence sensing of sulfamethazine. *Analyst* **2015**, *140*, 5301–5307. [[CrossRef](#)] [[PubMed](#)]

9. De Middeleer, G.; Dubruel, P.; De Saeger, S. Characterization of MIP and MIP functionalized surfaces: Current state-of-the-art. *TrAC Trends Anal. Chem.* **2016**, *76*, 71–85. [[CrossRef](#)]
10. Tang, L.; Zhao, C.Y.; Wang, X.H.; Li, R.S.; Yang, J.R.; Huang, Y.P.; Liu, Z.S. Macromolecular crowding of molecular imprinting: A facile pathway to produce drug delivery devices for zero-order sustained release. *Int. J. Pharm.* **2015**, *496*, 822–833. [[CrossRef](#)] [[PubMed](#)]
11. Wang, J.; Zhu, M.; Shen, X.; Li, S. A Cascade-Reaction Nanoreactor Composed of a Bifunctional Molecularly Imprinted Polymer that Contains Pt Nanoparticles. *Chem. Eur. J.* **2015**, *21*, 7532–7539. [[CrossRef](#)] [[PubMed](#)]
12. Li, J.; Zhang, L.; Wei, G.; Zhang, Y.; Zeng, Y. Highly sensitive and doubly orientated selective molecularly imprinted electrochemical sensor for Cu²⁺. *Biosens. Bioelectron.* **2015**, *69*, 316–320. [[CrossRef](#)] [[PubMed](#)]
13. Qian, K.; Deng, Q.; Fang, G.; Wang, J.; Pan, M.; Wang, S.; Pu, Y. Metal-organic frameworks supported surface-imprinted nanoparticles for the sensitive detection of metolcarb. *Biosens. Bioelectron.* **2016**, *79*, 359–363. [[CrossRef](#)] [[PubMed](#)]
14. Martín-Esteban, A. Recent molecularly imprinted polymer-based sample preparation techniques in environmental analysis. *Trends Environ. Anal. Chem.* **2016**, *9*, 8–14. [[CrossRef](#)]
15. Peng, H.; Luo, M.; Xiong, H.; Yu, N.; Ning, F.; Fan, J.; Chen, L. Preparation of photonic-magnetic responsive molecularly imprinted microspheres and their application to fast and selective extraction of 17 β -estradiol. *J. Chromatogr. A* **2016**, *1442*, 1–11. [[CrossRef](#)] [[PubMed](#)]
16. Arabi, M.; Ghaedi, M.; Ostovan, A. Development of dummy molecularly imprinted based on functionalized silica nanoparticles for determination of acrylamide in processed food by matrix solid phase dispersion. *Food Chem.* **2016**, *210*, 78–84. [[CrossRef](#)] [[PubMed](#)]
17. Yang, R.; Liu, Y.; Yan, X.; Liu, S.; Zheng, H. An Effective Method for the Synthesis of Yolk-Shell Magnetic Mesoporous Carbon-Surface Molecularly Imprinted Microspheres. *J. Mater. Chem. A* **2016**, *4*, 9807–9815. [[CrossRef](#)]
18. Barahona, F.; Díaz-Álvarez, M.; Turiel, E.; Martín-Esteban, A. Molecularly imprinted polymer-coated hollow fiber membrane for the microextraction of triazines directly from environmental waters. *J. Chromatogr. A* **2016**, *1442*, 12–18. [[CrossRef](#)] [[PubMed](#)]
19. Farid, M.M.; Goudini, L.; Piri, F.; Zamani, A.; Saadati, F. Molecular imprinting method for fabricating novel glucose sensor: Polyvinyl acetate electrode reinforced by MnO₂/CuO loaded on graphene oxide nanoparticles. *Food Chem.* **2016**, *194*, 61–67. [[CrossRef](#)] [[PubMed](#)]
20. Kong, X.; Gao, R.; He, X.; Chen, L.; Zhang, Y. Synthesis and characterization of the core-shell magnetic molecularly imprinted polymers (Fe₃O₄@MIPs) adsorbents for effective extraction and determination of sulfonamides in the poultry feed. *J. Chromatogr. A* **2012**, *1245*, 8–16. [[CrossRef](#)] [[PubMed](#)]
21. Yu, P.; Sun, Q.; Li, J.; Tan, Z.; Yan, Y.; Li, C. Magnetic imprinted nanomicrosphere attached to the surface of bacillus using miniemulsion polymerization for selective recognition of 2, 4, 6-trichlorophenol from aqueous solutions. *J. Ind. Eng. Chem.* **2015**, *29*, 349–358. [[CrossRef](#)]
22. Tan, L.; He, R.; Chen, K.; Peng, R.; Huang, C.; Yang, R.; Tang, Y. Ultra-high performance liquid chromatography combined with mass spectrometry for determination of aflatoxins using dummy molecularly imprinted polymers deposited on silica-coated magnetic nanoparticles. *Microchim. Acta* **2016**, *183*, 1469–1477. [[CrossRef](#)]
23. Arabi, M.; Ostovan, A.; Ghaedi, M.; Purkait, M.K. Novel strategy for synthesis of magnetic dummy molecularly imprinted nanoparticles based on functionalized silica as an efficient sorbent for the determination of acrylamide in potato chips: Optimization by experimental design methodology. *Talanta* **2016**, *154*, 526–532. [[CrossRef](#)] [[PubMed](#)]
24. Wu, Q.; Long, Q.; Li, H.; Zhang, Y.; Yao, S. An upconversion fluorescence resonance energy transfer nanosensor for one step detection of melamine in raw milk. *Talanta* **2015**, *136*, 47–53. [[CrossRef](#)] [[PubMed](#)]
25. Xue, J.; Lee, P.T.; Compton, R.G. Electrochemical detection of melamine. *Electroanalysis* **2014**, *26*, 1454–1460. [[CrossRef](#)]
26. Jawaid, S.; Talpur, F.N.; Sherazi, S.T.H.; Nizamani, S.M.; Khaskheli, A.A. Rapid detection of melamine adulteration in dairy milk by SB-ATR-Fourier transform infrared spectroscopy. *Food Chem.* **2013**, *141*, 3066–3071. [[CrossRef](#)] [[PubMed](#)]
27. Figueiredo, L.; Santos, L.; Alves, A. Synthesis of a Molecularly Imprinted Polymer for Melamine Analysis in Milk by HPLC with Diode Array Detection. *Adv. Polym. Technol.* **2015**, *34*. [[CrossRef](#)]

28. Pan, X.D.; Wu, P.G.; Yang, D.J.; Wang, L.Y.; Shen, X.H.; Zhu, C.Y. Simultaneous determination of melamine and cyanuric acid in dairy products by mixed-mode solid phase extraction and GC–MS. *Food Control* **2013**, *30*, 545–548. [[CrossRef](#)]
29. Lin, M.; He, L.; Awika, J.; Yang, L.; Ledoux, D.R.; Li, H.A.; Mustapha, A. Detection of melamine in gluten, chicken feed, and processed foods using surface enhanced Raman spectroscopy and HPLC. *J. Food Sci.* **2008**, *73*, T129–T134. [[CrossRef](#)] [[PubMed](#)]
30. Zhang, X.F.; Zou, M.Q.; Qi, X.H.; Liu, F.; Zhu, X.H.; Zhao, B.H. Detection of melamine in liquid milk using surface-enhanced Raman scattering spectroscopy. *J. Raman Spectrosc.* **2010**, *41*, 1655–1660. [[CrossRef](#)]
31. Miao, P.; Han, K.; Sun, H.; Yin, J.; Zhao, J.; Wang, B.; Tang, Y. Melamine functionalized silver nanoparticles as the probe for electrochemical sensing of clenbuterol. *ACS Appl. Mater. Interfaces* **2014**, *6*, 8667–8672. [[CrossRef](#)] [[PubMed](#)]
32. Cao, B.; Yang, H.; Song, J.; Chang, H.; Li, S.; Deng, A. Deng, Sensitivity and specificity enhanced enzyme-linked immunosorbent assay by rational hapten modification and heterogeneous antibody/coating antigen combinations for the detection of melamine in milk, milk powder and feed samples. *Talanta* **2013**, *116*, 173–180. [[CrossRef](#)] [[PubMed](#)]
33. Yan, X.; Li, H.; Li, Y.; Su, X. Visual and fluorescent detection of acetamiprid based on the inner filter effect of gold nanoparticles on ratiometric fluorescence quantum dots. *Anal. Chim. Acta* **2014**, *852*, 189–195. [[CrossRef](#)] [[PubMed](#)]
34. Yan, X.; Li, H.; Han, X.; Su, X. A ratiometric fluorescent quantum dots based biosensor for organophosphorus pesticides detection by inner-filter effect. *Biosens. Bioelectron.* **2015**, *74*, 277–283. [[CrossRef](#)] [[PubMed](#)]
35. Xu, S.; Lu, H. One-pot synthesis of mesoporous structured ratiometric fluorescence molecularly imprinted sensor for highly sensitive detection of melamine from milk samples. *Biosens. Bioelectron.* **2015**, *73*, 160–166. [[CrossRef](#)] [[PubMed](#)]
36. Wan, W.; Biyikal, M.; Wagner, R.; Sellergren, B.; Rurack, K. Fluorescent Sensory Microparticles that “Light-up” Consisting of a Silica Core and a Molecularly Imprinted Polymer (MIP) Shell. *Angew. Chem. Int. Ed.* **2013**, *52*, 7023–7027. [[CrossRef](#)] [[PubMed](#)]
37. Huy, B.T.; Seo, M.H.; Zhang, X.; Lee, Y.I. Selective optosensing of clenbuterol and melamine using molecularly imprinted polymer-capped CdTe quantum dots. *Biosens. Bioelectron.* **2014**, *57*, 310–316.
38. Zhou, Y.; Qu, Z.B.; Zeng, Y.; Zhou, T.; Shi, G. A novel composite of graphene quantum dots and molecularly imprinted polymer for fluorescent detection of paranitrophenol. *Biosens. Bioelectron.* **2014**, *52*, 317–323. [[CrossRef](#)] [[PubMed](#)]
39. Wang, J.; Qiu, H.; Shen, H.; Pan, J.; Dai, X.; Yan, Y.; Sellergren, B. Molecularly imprinted fluorescent hollow nanoparticles as sensors for rapid and efficient detection λ -cyhalothrin in environmental water. *Biosens. Bioelectron.* **2016**, *85*, 387–394. [[CrossRef](#)] [[PubMed](#)]
40. Li, L.; Lin, Z.Z.; Peng, A.H.; Zhong, H.P.; Chen, X.M.; Huang, Z.Y. Biomimetic ELISA detection of malachite green based on magnetic molecularly imprinted polymers. *J. Chromatogr. B.* **2016**, *229*, 403–408. [[CrossRef](#)] [[PubMed](#)]
41. Urraca, J.L.; Moreno-Bondi, M.C.; Orellana, G.; Sellergren, B.; Hall, A.J. Molecularly imprinted polymers as antibody mimics in automated on-line fluorescent competitive assays. *Anal. Chem.* **2007**, *79*, 4915–4923. [[CrossRef](#)] [[PubMed](#)]
42. Murase, N.; Taniguchi, S.I.; Takano, E.; Kitayama, Y.; Takeuchi, T. A molecularly imprinted nanocavity-based fluorescence polarization assay platform for cortisol sensing. *J. Mater. Chem. B.* **2016**, *4*, 1770–1777. [[CrossRef](#)]
43. Shi, S.; Guo, J.; You, Q.; Chen, X.; Zhang, Y. Selective and simultaneous extraction and determination of hydroxybenzoic acids in aqueous solution by magnetic molecularly imprinted polymers. *Chem. Eng. J.* **2014**, *243*, 485–493. [[CrossRef](#)]
44. Ni, Q.; Chen, B.; Dong, S.; Tian, L.; Bai, Q. Preparation of core–shell structure Fe₃O₄@SiO₂ superparamagnetic microspheres immobilized with iminodiacetic acid as immobilized metal ion affinity adsorbents for His-tag protein purification. *Biomed. Chromatogr.* **2016**, *30*, 566–573. [[CrossRef](#)] [[PubMed](#)]
45. Qiu, C.; Xing, Y.; Yang, W.; Zhou, Z.; Wang, Y.; Liu, H.; Xu, W. Surface molecular imprinting on hybrid SiO₂-coated CdTe nanocrystals for selective optosensing of bisphenol A and its optimal design. *Appl. Surf. Sci.* **2015**, *345*, 405–417. [[CrossRef](#)]
46. Hu, Y. Development of Innovative Biosensors for the Determination of Melamine in Milk. Master’s Thesis, The University of British Columbia, Vancouver, BC, Canada, 2015.

47. Chi, H.; Liu, B.; Guan, G.; Zhang, Z.; Han, M.Y. A simple, reliable and sensitive colorimetric visualization of melamine in milk by unmodified gold nanoparticles. *Analyst* **2010**, *135*, 1070–1075. [[CrossRef](#)] [[PubMed](#)]
48. DU, X.; Zhang, Y.; She, Y.; Liu, G.; Zhao, F.; Wang, J.; Wang, S.; Jin, F.; Shao, H.; Jin, M.; Zheng, L. Fluorescent competitive assay for melamine using dummy molecularly imprinted polymers as antibody mimics. *J. Integr. Agric.* **2016**, *15*, 1166–1177. [[CrossRef](#)]



© 2018 by the authors. Licensee MDPI, Basel, Switzerland. This article is an open access article distributed under the terms and conditions of the Creative Commons Attribution (CC BY) license (<http://creativecommons.org/licenses/by/4.0/>).